

# Characterizing Passively Q-switched Fiber Laser in LiDAR Application

Mahroof Mohamed Mafroos<sup>1</sup>, Nur Ameelia<sup>1</sup>, Husni Hani Jameela<sup>1</sup>, Azura Hamzah<sup>1\*</sup>

<sup>1</sup>Malaysia-Japan International Institute of Technology,  
Universiti Teknologi Malaysia, Jalan Sultan Yahya Petra, 54100 Kuala Lumpur, MALAYSIA

\*Corresponding Author

DOI: <https://doi.org/10.30880/ijie.2023.15.03.017>

Received 7 November 2022; Accepted 18 April 2023; Available online 15 August 2023

**Abstract:** A LiDAR system consists of a Q-switched fiber laser that emits light pulses to measure the distance from the target. We have experimentally demonstrated a passively Q-switched erbium-doped fiber laser (EDFL) by employing graphene saturable absorber (SA). The SA was prepared by dipping a polyvinyl alcohol (PVA) thin film into the graphene solution. Once the SA was fabricated, it can be placed in the cavity to perform pulses and it is operating at 1558.92 nm. The shortest pulse received is 3.9  $\mu$ s and generated at the repetition rate of 115 kHz. The pulses are stable between pump powers of 59.6mW and 127.1 mW. At the maximum pump power value of 127.1 mW, the laser cavity produced pulses with a 1.4mW output power and a 1.1nJ pulse energy.

**Keywords:** Graphene, carbon nanotube, Q-switching, saturable absorber, PVA / CNT

## 1. Introduction

Those short pulses can be produced from continuous wave (CW) or pulse wave (PW). Q-switching or mode locking systems can be used to produce a pulse laser. [1]. One of the advantages of pulsed fiber lasers is that they can produce exceptionally high peak powers from short pulses. [2]. Remote sensing, medical, military applications, material processing, and telecommunications are among potential applications for Q-switched fiber lasers. [3].

Light Detection and Ranging (LiDAR) technology is another key application of Q-switching. It's a method of remote sensing that employs light in the form of a pulsed laser to determine distances to the target in earth [4]. High frequency of Q-switched pulsed LiDAR is more precise and faster detection compared to conventional LiDAR. A conventional LiDAR can only measure up to 20-30 meters from the earth, however a Q-switched pulsed LiDAR can measure more than 30 meters [5]. Fig. 1 shows the typical block diagram of a LiDAR system.

By modulating the intra-cavity losses, the energetic short pulse laser is produced in Q-switching techniques [2]. The Q-switching technique is categorized into two, namely active and passive techniques. The passive Q-switching technique is easier to produce pulse waves due to compactness, simplicity, cost-effective and flexibility in design compared with active Q-switching [6]. An electro-optic-modulator or acousto-optic modulator should be used in an actively Q-switched pulses in laser [7], whereas, passive Q-switch does not require any external device. These extra modules in active Q-switching technique would cause unwanted loss in the cavity. However passively Q-switched fiber laser requires nonlinear absorption material called saturable absorber (SA) to produce pulse laser [8].

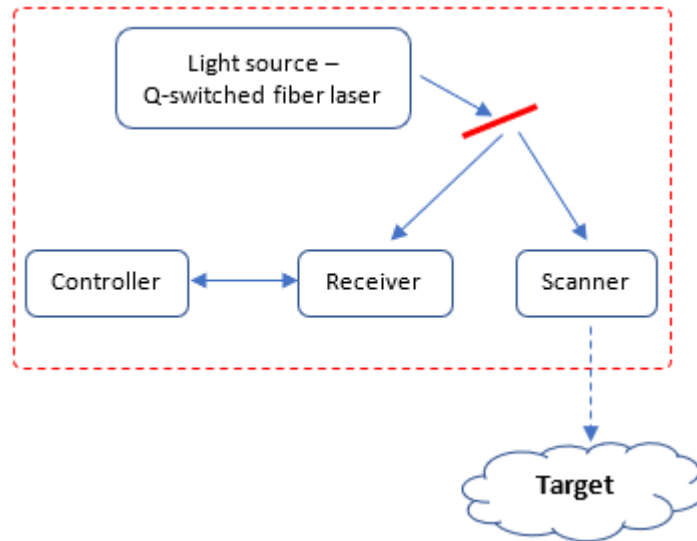


**Fig. 1 - LiDAR system [4]**

The semiconductor saturable absorption mirror (SESAM) is the first SA to generate pulse laser. The most common SAs utilized to receive Q-switched pulses were SESAMs and transition metal-doped (TMD) crystals.[9][10]. Due to certain disadvantages such as, complex fabrication and packaging which require costlier, narrowband operating bandwidth and need of additional optical components, SESAM is used rarely nowadays. TMD SA has gained a lot of interest in the realm of fiber lasers because of its distinctive energy band structure and optical properties. [11]. A variety of materials have been experimented as SA in a Q-switching techniques and provided favourable output, notably black phosphorus (BP), topological insulators (TIs) antimonene (Sb), tellurene (Te), carbon based SA namely graphene and carbon nanotubes (CNTs) and perovskite [7].

Graphene SA is utilized in this experiment to get better results in terms of pulse energy, output power, repetition rate, and pulse width. Graphene has outstanding linear and nonlinear optical properties, including its ultrafast recovery time, wavelength-independent SA range that spans the visible to mid-IR wavelength range[12], low threshold level of SA and intrinsic saturable absorption properties. Graphene is a 2D honeycomb lattice of carbon atoms that represents a single atomic layer of crystalline graphite [13]. Graphene is mechanically stable material due its mono-atomic structure[10]. Graphene is used as a SA in many applications involving antennas and other electronic devices have been used with conductive graphene[14]. It is possible to pattern an array of antenna, due to the graphene flake. It is big enough to support a series of metal electrodes. The resistivity of graphene is variable, and it decreases fast as the gate voltage rises [15].

Incorporation of an SA to a fiber laser cavity is done in different fabrication methods[16]. Fabrication of SA is one of the most important procedure to generate the pulse laser. Different methods are used to fabricate SA namely, evanescent wave coupling structure, thin film and polymer composite (sandwich structure), mechanical exfoliation, electrochemical exfoliation and drop cast techniques.

Some rare earth element doped in fiber to use as an active gain medium in fiber laser, namely Erbium (EDFL), Ytterbium (YDFL), Thulium (TDFL), Bismuth, Neodymium and Praseodymium (PDFL)[17]. EDFA is set as a gain medium in the ring cavity that incorporates graphene in a thin polyvinyl alcohol thin film as SA in this work.

## **2. Experimental Work – Graphene-PVA Saturable Absorber Fabrication Method**

In this experiment, the thin film and polymer composite method (sandwich structure) has been used to fabricate graphene SA. It is important to prepare PVA as a host polymer because of its excellence film forming, water solubility, transparently, non-toxicity, high durability and very high flexibility[2]. The commercialized ultra-high concentration graphene dispersion (Graphene supermarket CGD-100ML) SA was prepared by a cost-effective dip coating method as shown in Fig. 2 For 30 seconds, the PVA thin film is immersed in the graphene solution. The thickness, width and length of PVA thin film are 50µm, 1.5cm, 3cm. The volume of the graphene solution is 3ml. After that, the composite PVA-graphene solution was decanted into a petri dish and kept in a dry area for 2 days as shown in Fig. 3.

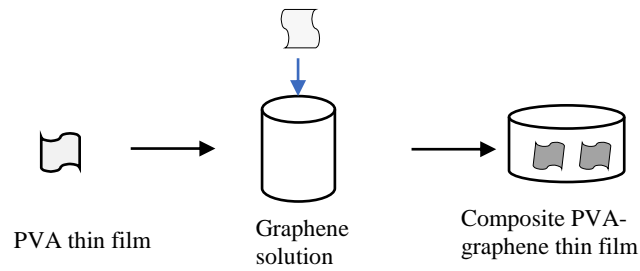


**Fig. 2 - Formation of thin film PVA-graphene SA**

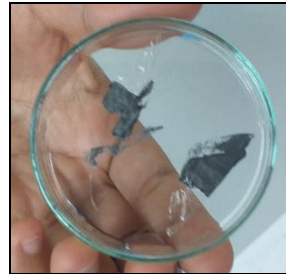


**Fig. 3 - PVA-graphene SA**

Once the SA is prepared, it is placed in between two fiber ferrules to form the SA in the 50 cm diameter of ring cavity as shown in Fig. 4. The sandwiching has been done using matching gel index. In this experiment, the SA is inserted between polarisation controller (PC) and gain medium.

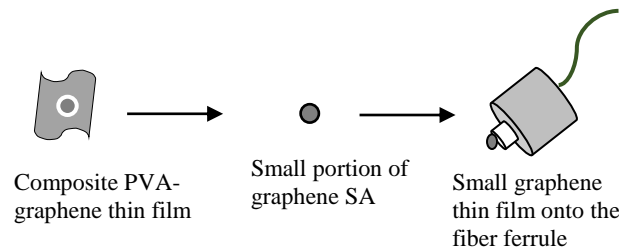


**Fig. 4 - Sandwiching graphene onto fiber ferrule**

## 2.1 Graphene-PVA Saturable Absorber Characterization

The graphene-PVA thin film was characterized using Raman spectroscopy. The Raman characterization in this experiment has been done using WiTec Alpha 300R Raman spectroscopy. The disorder arrangement in  $sp^2$  carbon structure in graphene is studied using Raman spectroscopy. The Raman spectra identifies the defect region (D) graphite region (G), and second-order Raman scattering (2D or G-) [18]. D-mode is caused by disordered structure of graphite material. The G-mode is raised, due to phonon vibrations in the material. The spectroscopy image of graphene is shown in

Fig. 5 (a) and the graphene's Raman spectrum is shown in

Fig. 5 (b).

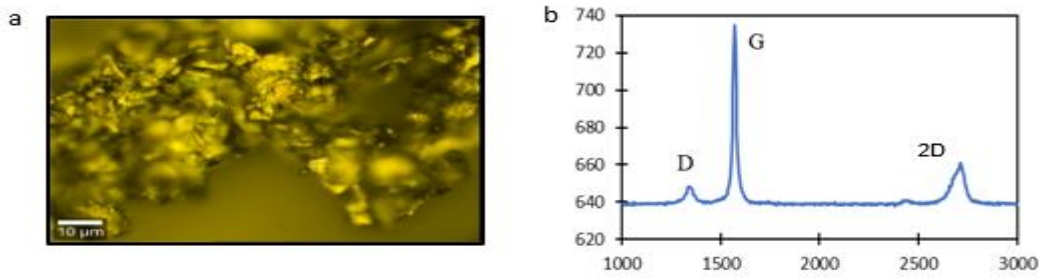


**Fig. 5 - Raman spectroscopy (a) image; (b) spectrum of graphene**

The crystallinity of the film is reflected in the strong peaks in the Raman spectrum. The spectrum shows D, G, and 2D bands for graphene at 1345 cm<sup>-1</sup>, 1570 cm<sup>-1</sup>, 2708 cm<sup>-1</sup>, respectively.

## 2.2 Experimental Set-Up

Fig. 6 depicts the experimental setup for the Q-switching techniques using a 1.7 m EDF and function as gain medium. A 980/1550 nm wavelength division multiplexer (WDM), and a 95/5 output coupler are also connected in a ring cavity. The fabricated graphene SA is placed between two fiber ferrules. A 980 nm laser diode pumped the EDF through the WDM. An optical isolator is placed, so that no backward reflection will occur. The optical spectrum analyzer (OSA) with and without SA was used to examine the spectrum of the EDFL. The output pulse was inspected by using oscilloscope (OSC).

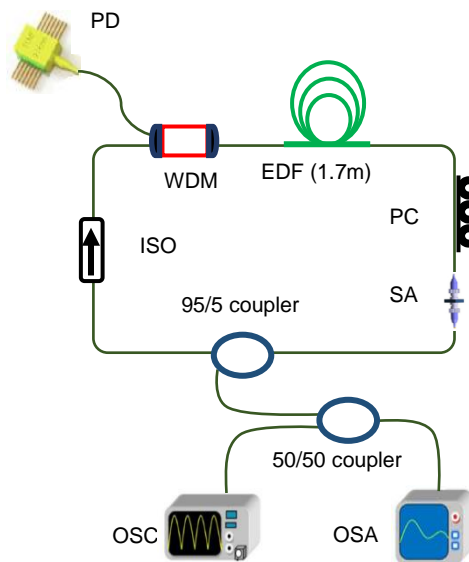


**Fig. 6 - Experimental Setup for Q-switched EDFA**

## 3. Results and Discussion

The pump power is slowly increased to obtain the pulse lasing threshold for Q-switching operation. At 59.6 mW pump power, the pulse laser began to operate and diminished lasing the pulse laser beyond the pump power of 127.1 mW. Fig. 7 depicts the laser's optical spectrum with and without SA integration.

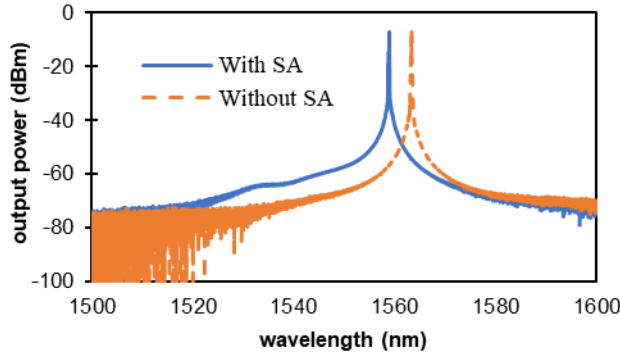


**Fig. 7 - OSA trace with and without SA**

The Q-switched pulse laser generates at 1558.92 nm and the continuous wave (without the SA) operates at 1563.27nm. This has shown that the Q-switched laser operating wavelength has become a shorter wavelength. This is due to the cavity loss, which is bigger when combined with the SA, causing the oscillation wavelength to be reduced to achieve a higher gain. Because of this, the signal in the cavity has become a shorter wavelength.

The repetition rates in kilo Hertz (kHz) and pulse widths in micro seconds ( $\mu$ s) against the pump power has been observed and the plotted graph is shown in Fig. 8. As shown in the figure, when the pump power is increased, the repetition rate of the pulse is increased and the pulse width is decreased. The pulse laser is steady when the pump power is set between 59.6 and 127.1 mW and the pulse repetition rate is varying from 74 to 115 kHz and pulse width is varying from 6.1 to 3.9 $\mu$ s. So the shortest pulse width is achieved when the pump power is maximum.

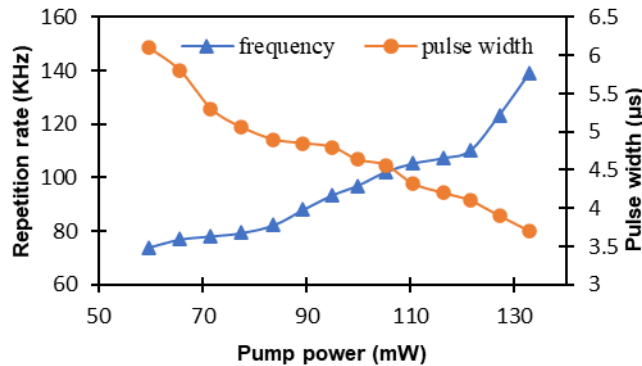


**Fig. 8 - Repetition rate and pulse width as a function of input pump power**

Fig. 9 plots the pulse energy and output power for the EDFL connect with 980 nm pumping against pump power. The pump power increases the both pulse energy and output power. The highest output power and highest pulse energy are 1.4 mW and 12.17n J, respectively, at 127.1 mW pump power. Compare to some of the previous studies using other SA materials, notably SWCNT[6], MoS<sub>2</sub> [19], gold nano bipyramids [20] and titanium dioxide [7], graphene SA shows promising potential output results.

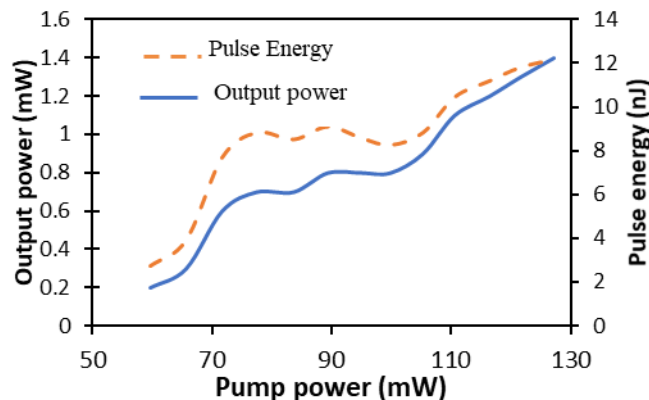


**Fig. 9 - Peak power and pulse energy against pump power**

It is observed that at the threshold pump power is 59.6 mW, the proposed experiment generates a steady Q-switching pulse with a repetition rate of 79.37 kHz and pulse width of 5.06  $\mu\text{s}$  as shown in Fig. 10. The oscilloscope trace is to detect and confirmed that the presence of fiber laser.

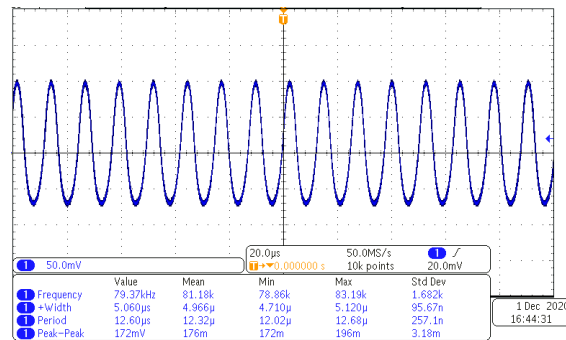


Fig. 10 - Pulse train of Q-switching operation

#### 4. Conclusion

Using a graphene SA, an experiment of a passively Q-switched EDFL was successfully experimented. The pulse laser output is as discussed, and instantaneous peak power and pulse energy are highly created. In this research, graphene-PVA SA was used to generate pulse laser due to its advantages over other material. The highest output power was 1.4 mW and single pulse energy was 12.17 n J, and the minimal pulse width of 3.9 $\mu\text{s}$  for 115 kHz repetition rate. The results of our experiments clearly showed that graphene can be employed as a saturable absorber for LiDAR technology at 1.55  $\mu\text{m}$  wavelength.

#### Acknowledgement

The author would like to thank Universiti Teknologi Malaysia and Ministry of Higher Education under the Fundamental Research Grant Scheme (FRGS) number: R. K130000.7843.5F350 for funding this project.

#### Reference

- [1] R. A. M. Yusoff *et al.*, "Q-switched and mode-locked erbium-doped fiber laser using gadolinium oxide as saturable absorber," *Opt. Fiber Technol.*, vol. 57, no. April, 2020, doi: 10.1016/j.yofte.2020.102209.
- [2] S. A. Sadeq, S. K. Al-Hayali, S. W. Harun, and A. Al-Janabi, "Copper oxide nanomaterial saturable absorber as a new passive Q-switcher in erbium-doped fiber laser ring cavity configuration," *Results Phys.*, vol. 10, no. April, pp. 264–269, 2018, doi: 10.1016/j.rinp.2018.06.006.
- [3] X. Rong *et al.*, "919.8 nm self-Q-switched Nd-doped silica all-fiber laser," *Opt. Commun.*, vol. 473, no. April, p. 125939, 2020, doi: 10.1016/j.optcom.2020.125939.
- [4] H. A. O. Wakati *et al.*, "[hao wakati mwingin kau tonut," vol. 1, 2017.
- [5] S. W. Harun, "Ultrafast Photonics and High Power Lasers," 2020.
- [6] M. Z. Zulkifli *et al.*, "Tunable passively Q-switched ultranarrow linewidth erbium-doped fiber laser," *Results Phys.*, vol. 16, no. November 2019, pp. 0–5, 2020, doi: 10.1016/j.rinp.2020.102949.
- [7] N. M. Yusoff *et al.*, "Low threshold Q-switched fiber laser incorporating titanium dioxide saturable absorber from waste material," *Optik (Stuttg.)*, p. 164998, 2020, doi: 10.1016/j.ijleo.2020.164998.
- [8] M. T. Ahmad, A. R. Muhammad, R. Zakaria, H. Ahmad, and S. W. Harun, "Electron beam deposited silver (Ag) saturable absorber as passive Q-switcher in 1.5- and 2-micron fiber lasers," *Optik (Stuttg.)*, vol. 207, no. December 2019, p. 164455, 2020, doi: 10.1016/j.ijleo.2020.164455.
- [9] X. Zhu and S. Chen, "Study of a graphene saturable absorber film fabricated by the optical deposition method," *IEEE Photonics J.*, vol. 11, no. 6, pp. 1–9, 2019, doi: 10.1109/JPHOT.2019.2948940.
- [10] H. Ahmad, M. Z. Samion, A. S. Sharbirin, and M. F. Ismail, "Dual-wavelength, passively Q-switched thulium-doped fiber laser with N-doped graphene saturable absorber," *Optik (Stuttg.)*, vol. 149, pp. 391–397, 2017, doi: 10.1016/j.ijleo.2017.09.054.
- [11] K. Zhang *et al.*, "Passively Q-switched pulsed fiber laser with higher-order modes," *Infrared Phys. Technol.*, vol. 105, no. November 2019, p. 103163, 2020, doi: 10.1016/j.infrared.2019.103163.
- [12] J. Liu, J. Xu, and P. Wang, "Graphene-based passively Q-switched 2  $\mu\text{m}$  thulium-doped fiber laser," *Opt. Commun.*, vol. 285, no. 24, pp. 5319–5322, 2012, doi: 10.1016/j.optcom.2012.07.063.
- [13] L. Ding, B. Xu, C. Xu, J. Huang, and D. Guo, "Preparation and Saturable Absorption Property of Graphene on the

- Optic Fiber Side by Transferring CVD-Graphene Grown on Ni,” *IOP Conf. Ser. Mater. Sci. Eng.*, vol. 230, no. 1, 2017, doi: 10.1088/1757-899X/230/1/012029.
- [14] S. N. F. Zuikafly, A. Khalifa, F. Ahmad, S. Shafie, and S. W. Harun, “Conductive graphene as passive saturable absorber with high instantaneous peak power and pulse energy in Q-switched regime,” *Results Phys.*, vol. 9, no. March, pp. 371–375, 2018, doi: 10.1016/j.rinp.2018.03.002.
- [15] M. Dragoman, A. A. Muller, D. Dragoman, F. Coccetti, and R. Plana, “Terahertz antenna based on graphene,” *J. Appl. Phys.*, vol. 107, no. 10, pp. 1–4, 2010, doi: 10.1063/1.3427536.
- [16] Y. I. Hammadi and T. S. Mansour, “A Simple and Efficient Method to Fabricate Graphene 2D Nanomaterial into a thin Film to Serve as a Saturable a bsorber for Fiber Laser Application,” *Int. J. Eng. Technol.*, vol. 7, no. 4.15, p. 298, 2018, doi: 10.14419/ijet.v7i4.15.23011.
- [17] N. A. Awang, N. S. Aziz, A. N. Azmi, F. S. Hadi, and Z. Zakaria, “Experimental and Numerical Comparison Q-Switched Fiber Laser Generation using Graphene as Saturable Absorber,” *MATEC Web Conf.*, vol. 150, 2018, doi: 10.1051/mateconf/201815001009.
- [18] D. A. Note and F. Transform, “Discover the Raman Advantage !,” *Energy*, no. 866, pp. 82070–82070, 2000.
- [19] B. Chen, X. Zhang, K. Wu, H. Wang, J. Wang, and J. Chen, “Q-switched fiber laser based on transition metal dichalcogenides MoS<sub>2</sub>, MoSe<sub>2</sub>, WS<sub>2</sub>, and WSe<sub>2</sub>,” *Opt. Express*, vol. 23, no. 20, p. 26723, 2015, doi: 10.1364/oe.23.026723.
- [20] W. Zhang *et al.*, “Gold nanobipyramids as a saturable absorber for passively Q-switched Er<sup>3+</sup>: ZBLAN fiber laser,” *Opt. Laser Technol.*, vol. 111, no. April 2018, pp. 30–34, 2019, doi: 10.1016/j.optlastec.2018.09.020.